Supplementary Information (SI) for Soft Matter.
This journal is © The Royal Society of Chemistry 2025

# Diffusive evaporation dynamics in polymer solutions is ubiquitous - Supplemental Information

Max Huisman,[1] Wilson C. K. Poon,[1] Patrick B. Warren,[1,2] Simon Titmuss,[1] and Davide Marenduzzo[1]

[1] *SUPA, School of Physics and Astronomy, University of Edinburgh, Peter Guthrie Tait Road, Edinburgh EH9 3FD, United Kingdom*

[2] *The Hartree Centre, STFC Daresbury Laboratory, Warrington WA4 4AD, United Kingdom*

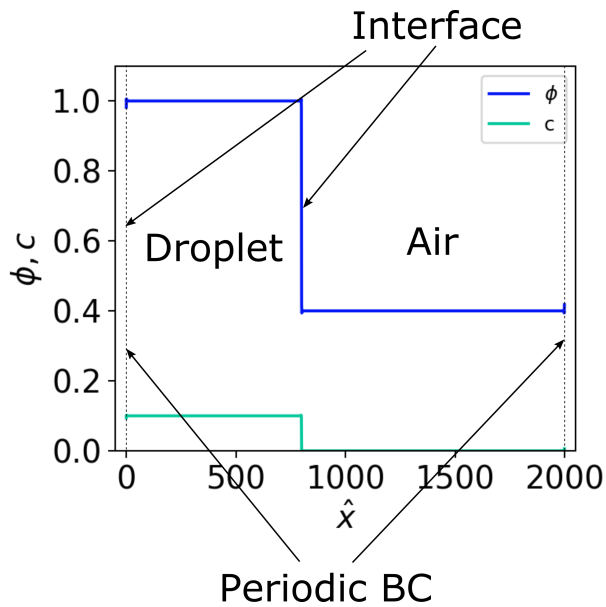


FIG. 1. Initialized one dimensional system, where $\phi$ and $c$ are piecewise continuous over the simulation domain. The droplet and the surrounding air phases are separated by an interface, which is smooth during the dynamics. Here 2/5 of the system is droplet and the remainder is air.

## I. ANALYTICAL MODEL

### A. Set-up of the Analytical System

For the binary polymer-water system we create two fields, one (the phase field) for the total mass of the droplet $\phi$, and one for the polymer concentration $c$, which is essentially non-zero only inside the droplets. The two fields are discretized over the same 1D lattice, so that each lattice contains some finite value of $\phi$ and $c$.

We initialize a system with two phases, the droplet and the surrounding air, separated by an interface, see for example Fig. 1. In phase 1, inside the droplet, we initialize $\phi = \phi_1$ $(= 1)$ and $c$ to some other finite value $c = c_0$, where $c_0 < \phi_1$. In phase 2, the surrounding air, we initialize $c = 0$ and $\phi = \phi_0$ with $\phi_0 < \phi_1$, which then qualitatively represents the Relative Humidity (RH).

Since the amount of solvent in the air phase should not significantly increase during a simulation, as in reality would also not happen to the environment during evaporation, we can safely allow $\phi$ not to be conserved in the surrounding phase.

Furthermore, we used periodic boundary conditions, which means in the case of the one-dimensional droplet there are two interfaces between the droplet and the air.

### B. Applying Cahn-Hilliard to Evaporation of a Binary Polymeric Mixture

We start from the general Cahn-Hilliard expression for $\phi$ and add a convective term to account for the advective flux driven by evaporation, similar to [1]. We consider the following equation for the phase field $\phi$:

$$\frac{\partial \phi(x,t)}{\partial t} + v_i \nabla \cdot \phi = M_\phi \nabla \cdot \left[ \nabla \frac{\delta F}{\delta \phi(x)} \right] . \tag{1}$$

In this form, the phase field is not conserved as its time derivative does not equal a total divergence. This is due to the $v_i \cdot \nabla \phi$ term. We express the interfacial velocity as $v_i = \gamma \nabla (\phi - \frac{\gamma'}{\gamma} c)$, where $\gamma'$ and $\gamma$ are kinetic parameters. This phenomenological form is chosen because the driving force for evaporation – hence for the motion of the gas/droplet boundary – is provided by gradients in the water activity (in our model phenomenologically represented by $\nabla \phi$), which decreases with polymer concentration $c$. The ratio $\frac{\gamma'}{\gamma}$ gives the extent to which the polymer reduces the evaporation rate. Using an alternative form for the evaporation rate, that for instance depends on the local value of $\phi$ as $v_i' = \phi \times \gamma \nabla (\phi - \frac{\gamma'}{\gamma} c)$, gives nearly identical results for the interface shrinkage $\Delta x_i$, settling in Diffusion-Limited Evaporation (DLE), Fig. 2. Finally, we use the fact that $\frac{\delta F}{\delta \phi} = \mu_\phi$ and assume that the mobility $M_\phi$ is constant. This leads to the following governing equation for the phase field $\phi$:

$$\frac{\partial \phi(x,t)}{\partial t} + v_i \cdot \nabla \phi = M_\phi \nabla^2 \mu_\phi \, . \tag{2}$$

We also require an equation for the polymer field, which reads:

$$\frac{\partial c(x,t)}{\partial t} + \nabla \cdot (vc) = \nabla \cdot (M_c(c) \nabla \mu_c) \, , \tag{3}$$

where $c$ is conserved globally and we assume that the mobility of the polymer is dependent on $c$ as $M(c) = \frac{M_0}{1+\beta c}$. The polymer experiences a velocity $v = -v_i$, which is the water velocity that advects the polymer towards the interface.

Note that, another possible interpretation could be of $\phi$ and $c$ as solvent and polymer concentration, respectively. In that case the system would effectively be compressible where there is an increase of $c$ inside the drop. Since the total concentration of material (polymer

and solvent) is equal to $\phi + Ac$, where $A$ is a proportionality constant which is not strictly defined, compressibility can be made negligible for small $A$.

The form of the solvent velocity $v$, and equivalently of the interfacial velocity $v_i$, can also be derived by noting that the force driving solvent flow in the Navier-Stokes equation is $-\nabla p$, with $p$ the pressure of water, which decreases with polymer concentration. As we only use a 1d effective theory, a detailed derivation of the flow field is outside the scope of the current work.

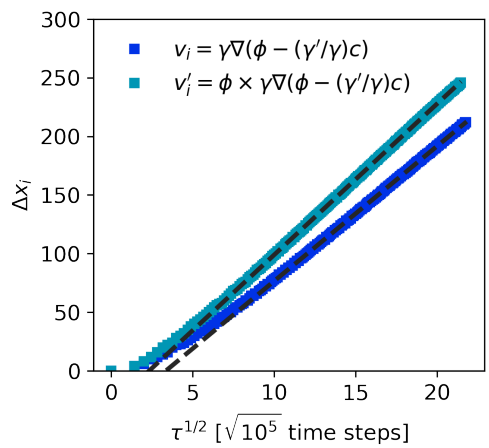


FIG. 2. Comparison of mass loss $\Delta x_i(t)$ vs $t^{1/2}$ for the evaporation rate expressions $v_i = \gamma\nabla(\phi - \frac{\gamma'}{\gamma}c)$ and $v_i' = \phi \times \gamma\nabla(\phi - \frac{\gamma'}{\gamma}c)$. Both simulations use the exact same parameters for the free energy density $f(\phi, c)$, with $\phi_0 = 0.4$ and $\gamma'/\gamma = 1.5$. Striped black lines are linear fits to $t^{1/2}$.

### C. Free Energy Density and Chemical Potentials

To obtain the diffusive term we calculate the chemical potentials as functional derivatives of the free energy density, that depends on the local values of $\phi$ and $c$:

$$\mu_\phi = \frac{\delta F}{\delta \phi} = \frac{\partial f}{\partial \phi} - \nabla \cdot \frac{\partial f}{\partial \nabla \phi}\,, \tag{4a}$$

$$\mu_c = \frac{\delta F}{\delta c} = \frac{\partial f}{\partial c} - \nabla \cdot \frac{\partial f}{\partial \nabla c}\,. \tag{4b}$$

We start from the following functional form for $f$:

$$f = \frac{a_1}{4}(\phi - \phi_0)^2(\phi - \phi_1)^2 + \frac{\kappa_\phi}{2}(\nabla\phi)^2 + \frac{\kappa_c}{2}(\nabla c)^2 - \frac{a_0}{2}\phi^2 c^2 + \frac{b_0}{2}c^2 + \frac{b_1}{4}c^4 \tag{5}$$

Here, the first term $\frac{a_1}{4}(\phi-\phi_0)^2(\phi-\phi_1)^2$ drives phase separation into two phases of compositions $\phi_1$ and $\phi_0$; the second and third terms $\frac{\kappa_\phi}{2}(\nabla\phi)^2$ and $\frac{\kappa_c}{2}(\nabla c)^2$ give the bare surface tension of $\phi$ and $c$; the fourth term $\frac{a_0}{2}\phi^2c^2$ is a phase field phenomenological term which favours the internalisation of the polymer inside the droplet; the fifth term $\frac{b_0}{2}c^2$ represents the virial coefficient for polymer diffusion; and the final term $\frac{b_1}{4}c^4$ is the excluded volume interaction of the polymer.

### D. Energy Penalty for Polymer Evaporation

The phase field model as outlined in the above is purely interaction based through the free energy density equation. Since polymer and solvent have affinity, in the current form of Eq. 10 polymer will 'leak' into the outer phase. This is not physically unrealistic in liquid-liquid systems, but will become an issue when there is a phase change over the interface like in a gas-liquid system.

In a gas-liquid system, solvent molecules are easily transferred to the gas phase, *e. g.* this does not require much energy. Thus, the energy contribution for $\phi$ to cross the interface and move from liquid to gas can be safely ignored in Eq. 10.

The solute is involatile and unlikely to evaporate, so there should be an energy penalty for $c$ to cross the interface to the outer phase $\phi_0$. This can be implemented by adding a term $g(x)\frac{a_2}{2}c^2$ to our free energy density so that it becomes

$$f(\phi,c)=\frac{a_1}{4}(\phi-\phi_0)^2(\phi-\phi_1)^2+\frac{\kappa_\phi}{2}|\nabla\phi|^2+\frac{\kappa_c}{2}|\nabla c|^2-\frac{a_0}{2}\phi^2c^2+g(x)\frac{a_2}{2}c^2+\frac{b_0}{2}c^2+\frac{b_1}{4}c^4\,, \quad (6)$$

where $g(x)=\Theta(\phi(x)-\frac{\phi_1-\phi_0}{2})$ is an indicator function which is zero if $\frac{\phi_1-\phi_0}{2}>\phi(x)$ and one otherwise, and $a_2$ is the energy penalty (units $E/L^2$) for the polymer to be in the outer phase.

### E. Concentration Cap

When $c$ increases to some concentration $c=c_g$, the polymer gels and contributes a permanent elastic stress to the system [2, 3]. This effect can be implemented into the free energy by adding a term $G(x)\frac{K_\mathrm{g}}{2}(c(x)-c_\mathrm{g})^2$, which now becomes

$$f(\phi,c)=\frac{a_1}{4}(\phi-\phi_0)^2(\phi-\phi_1)^2+\frac{\kappa_\phi}{2}|\nabla\phi|^2+\frac{\kappa_c}{2}|\nabla c|^2-\frac{a_0}{2}\phi^2c^2+g(x)\frac{a_2}{2}c^2+G(x)\frac{K_\mathrm{g}}{2}(c-c_\mathrm{g})^2+\frac{b_0}{2}c^2+\frac{b_1}{4}c^4\,, \quad (7)$$

where $G(x) = \Theta(c(x) - c_{\mathrm{g}})$ is another indicator function which is zero if $c(x) < c_{\mathrm{g}}$ and one otherwise, and $K_{\mathrm{g}}$ (units $E/L^2$) is the osmotic bulk modulus in the gel phase.

### F. Chemical Potential Expressions

The chemical potentials used in the diffusive term read as follows:

$$\mu_\phi = \frac{\partial f}{\partial \phi} - \nabla \cdot \frac{\partial f}{\partial \nabla \phi} = a_1(\phi - \phi_0)(\phi - \phi_1)(\phi - \frac{\phi_0 + \phi_1}{2}) - a_0 c^2 \phi - \kappa_\phi \nabla^2 \phi \,, \tag{8a}$$

$$\mu_c = \frac{\partial f}{\partial c} - \nabla \cdot \frac{\partial f}{\partial \nabla c} = -a_0 c \phi^2 + b_0 c + g(x) a_2 c + b_1 c^3 + G(x) K_{\mathrm{g}}(c - c_{\mathrm{g}}) - \left[\kappa_c \nabla^2 c\right] \,. \tag{8b}$$

### G. Parameter values

Since the phase field equations are not derived from coarse graining a microscopic model, we need to choose all phenomenological parameters such that the system behaves realistically. The set of parameters that was used in our simulations for the free energy and the conservation equations, in units of $E$ (energy $\delta E$), $L$ (length $\delta x$) and T (time $\delta t$), is given in Table I.

TABLE I. Parameter values used in simulations.

| Parameter | Units | Value |
|---|---|---|
| $a_1$ | $E/L^3$ | 1.0-3.0 |
| $\kappa_\phi$ | $E/L$ | 0.1 |
| $\kappa_c$ | $E/L$ | 0.1-0.4 |
| $a_0$ | $E/L^3$ | 0.02 |
| $b_0$ | $E/L^3$ | 0.001-0.03 |
| $b_1$ | $E/L^3$ | 0.001 |
| $\gamma$ | $L^2/T$ | 0.0001 |
| $\gamma'$ | $L^2/T$ | 0.00005-0.0003 |
| $M_\phi$ | $L^3L^2/ET$ | 0.1 |
| $M_0$ | $L^3L^2/ET$ | 0.025-0.1 |
| $\beta$ | - | 0.5-5.0 |
| $a_2$ | $E/L^3$ | 0.5 |
| $K_{\mathrm{g}}$ | $E/L^3$ | 0.5 |
| $c_{\mathrm{g}}$ | - | 0.5-1.0 |

### H. Computational Methods

To solve the system Eq. 2, Eq. 3 and Eqs. 8, we used a Lattice-Boltzmann implementation in $C$ that iterates through the following steps:

1. Calculate gradients of $\phi$ and $c$ in space using finite difference methods

$$\partial f/\partial x = \frac{f(x+h) - f(x-h)}{2h},$$
$$\partial^2 f/\partial x^2 = \frac{f(x+h) - f(x-h) - 2f(x)}{h^2};$$

2. Calculate $\mu_\phi(x)$ and $\mu_c(x)$ using Eqs. 8;

3. Calculate $v_i = \gamma\nabla(\phi - \frac{\gamma'}{\gamma}c)$ and gradients in $\mu_\phi(x)$ and $\mu_c(x)$ using finite difference;

4. Calculate $\phi_{\text{new}}(x)$ and $c_{\text{new}}(x)$ using Eq. 2 and Eq. 3, and update the system.

## II. STABILITY FOR INITIAL CONDITIONS

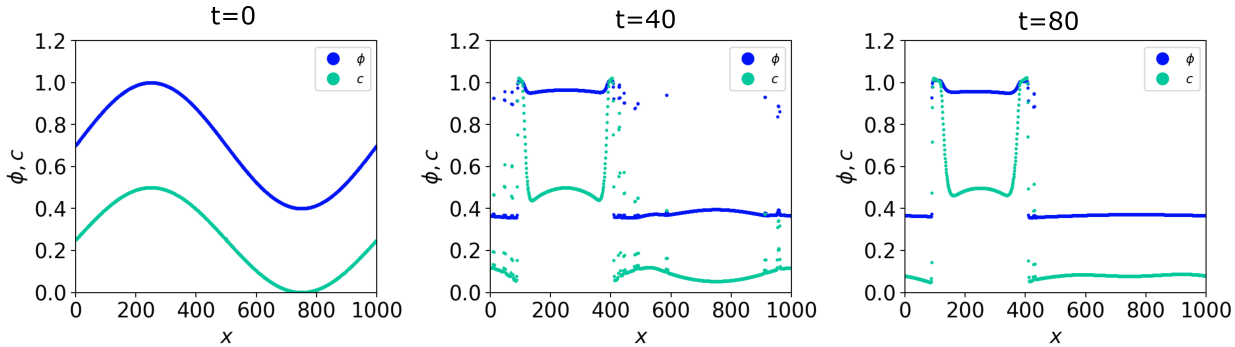


FIG. 3. Early times evolution of the profiles of $\phi$ and $c$, initialized using sinusoidal initial conditions Eq. 9a and Eq. 9b.

The functional form of Eq. 7 suggests that the system should spontaneously phase separate into a droplet phase and into an environment phase, which entails that the dynamics in the system should be independent of the initial conditions. We test this hypothesis by initializing a one-dimensional system with a sinusoidal distribution of $\phi$ and $c$ as:

$$\phi(x, t = 0) = \frac{\phi_1 - \phi_0}{2} \times [\sin(2\pi x/L_x) + 1] + \phi_0 \,, \tag{9a}$$

$$c(x, t = 0) = \frac{c_0}{2} \times [\sin(2\pi x/L_x) + 1] \,, \tag{9b}$$

with $L_x$ the total system size, as shown in Fig. 3. Using parameters from the range in Table I, after a short initializiation period in which small droplets form in the air phase, Fig. 3 ($t = 40$), we quickly retrieve a similar concentration profile to Fig. 1b in the main manuscript, Fig. 3 ($t = 80$). In the long times regime, the familiar mass loss scaling $m(t) \sim \Delta x_i(t) \sim t^{1/2}$ is observed, Fig. 4.

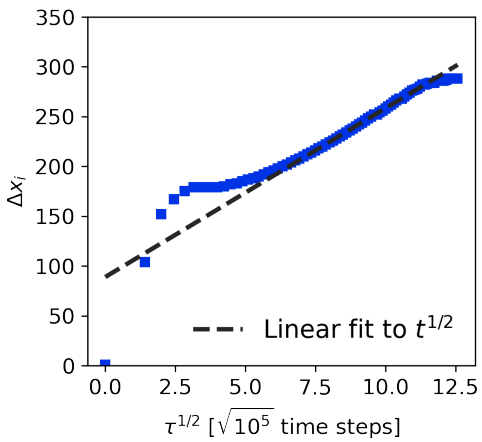


FIG. 4. Evolution of $m(t) \sim \Delta x_i(t) \sim t^{1/2}$ for system initialized using sinusoidal initial conditions Eq. 9a and Eq. 9b. Linear fit to $t^{1/2}$ is provided to highlight the settling in DLE.

## III. FLORY-HUGGINS IMPLEMENTATION IN THE MODEL

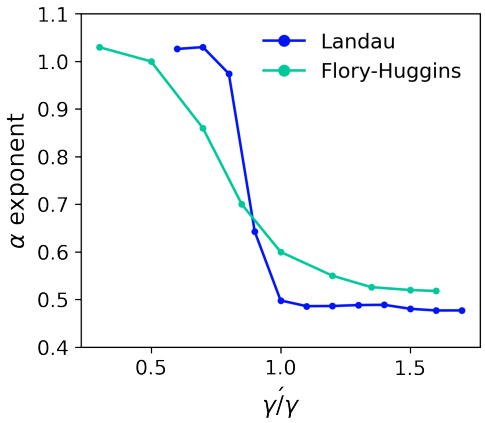


FIG. 5. Comparison of the evolution of the time exponent $\alpha$ between the Laundau and Flory-Huggins models of the polymeric free energy density, with varying $\gamma'/\gamma$ and $\phi_0 = 0.40$. Other simulation settings for the Flory-Huggins implementation: $b_0 = 0.02$ and $\chi = 0.001$.

We show how our model can be adapted to using a different polymer model by replacing the Landau expansion for the free energy by a Flory-Huggins model. For large degree of polymerization $N \gg 1$, the free energy density equation becomes:

$$f(\phi, c) = \frac{a_1}{4}(\phi - \phi_0)^2(\phi - \phi_1)^2 + \frac{\kappa_\phi}{2}|\nabla\phi|^2 + \frac{\kappa_c}{2}|\nabla c|^2 - \frac{a_0}{2}\phi^2 c^2 + g(x)\frac{a_2}{2}c^2 + G(x)\frac{K_{\mathrm{g}}}{2}(c - c_{\mathrm{g}})^2 + b_0(1-c)\ln(1-c) + \chi c(1-c)\,. \tag{10}$$

Therefore, neglecting any constant contributions, the chemical potential for the polymer now reads:

$$\mu_c = \frac{\partial f}{\partial c} - \nabla\cdot\frac{\partial f}{\partial \nabla c} = -a_0 c\phi^2 - b_0\ln(1-c) + g(x)a_2 c + \chi(1-2c) + G(x)K_{\mathrm{g}}(c - c_{\mathrm{g}}) - \left[\kappa_c \nabla^2 c\right]\,. \tag{11}$$

The solvent chemical potential remains unchanged.

We compare implementations using a Landau expansion and a Flory-Huggins expression in one line from the state diagrams in Fig 2 of the main manuscript, for varying $\gamma'/\gamma$ and constant $\phi_0 = 0.4$, in Fig. 5. Other simulation settings for the Flory-Huggins implementation are $b_0 = 0.02$ and $\chi = 0.001$. Whilst the behaviour is qualitatively the same, a quantitative difference is observed, where the transition from $m(t) \sim t^1$ to $m(t) \sim t^{1/2}$ is less sharp in using the Flory Huggins equation. We explain this difference through the divergence of $b_0 \ln(1-c)$ for $c \to 1$, meaning that there is more spreading near the interface at high $c$ which should lead to slight variations in the settling interface concentration $c_i$, that depend on the driving force, set by $\phi_0$.

## IV. EVAPORATION RATE AND GROWTH OF POLYMER LAYER

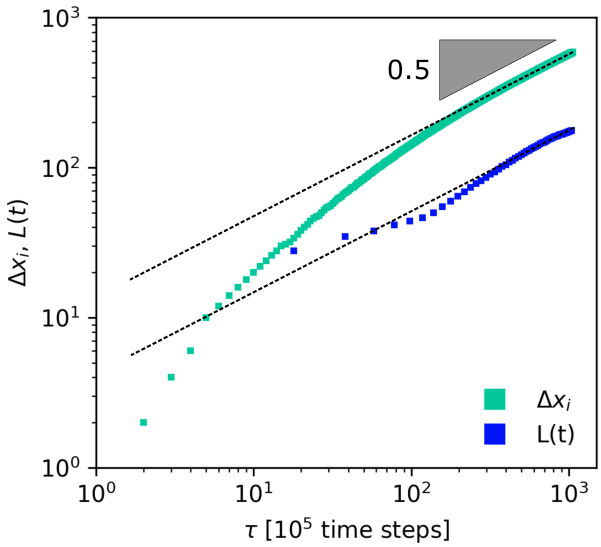


FIG. 6. Comparison of the evolution of the interface $\Delta x_\mathrm{i}$ and the polymer layer thickness $L(t)$ in a system with $\gamma'/\gamma = 1.5$ and $\phi_0 = 0.35$, plotted logarithmically to highlight the long time power-law behaviour. The capping concentration is reached after approximately $t = 100$ timesteps.

Our physical interpretation of the DLE regime is that it is due to the buildup of polymer at the interface. After the polymer concentration at the interface has reached $c = c_\mathrm{g}$, the polymer layer grows inward as it is swept up by the shrinking interface into the droplet as water molecules diffuse outwards to evaporate. Physically, we therefore expect the scaling law $L(t) \sim m(t)$ to hold, where $L(t)$ is the Full Width Half Maximum (FWHM) of the peak in $c$ near the interface and $m(t)$ is the mass loss.

To test this scaling law we look at the exponents of the mass loss, e.g. the interface shrinkage $\Delta x_\mathrm{i}$, $m(t) \sim \Delta x_\mathrm{i} \sim t^\alpha$ and the polymer layer growth $L(t) \sim t^\beta$ in an evaporating droplet where the polymer reaches its capping/gel concentration early in the simulation (Fig. 6). We determine the time exponents $\alpha = 0.56$ and $\beta = 0.60$ by power-law fitting, which are indeed similar.


[1] H. G. Lee, J. Yang, S. Kim, and J. Kim, Appl. Math. Comput. **390**, 125591 (2021).

[2] L. Leibler and K. Sekimoto, Macromol. **26**, 6937 (1993).

[3] T. Okuzono and M. Doi, Phy. Rev. E **77**, 030501(R) (2008).